Optimized planar dividing surfaces for asymmetric activated-rate processes

Anatoli M. Frishman, Alexander M. Berezhkovskii,* and Eli Pollak
Chemical Physics Department, Weizmann Institute of Science, Rehovot, 76100, Israel
(Received 27 October 1993)

The variational-transition-state theory (VTST) approach to condensed-phase activated-rate processes is extended to include bent planar dividing surfaces. This allows removal of formal divergences which arise when applying VTST, based on simple planar dividing surfaces, to unrestricted potentials. Practical applications are demonstrated for the cubic and strongly asymmetric quartic potentials.

PACS number(s): 05.40.+j

I. INTRODUCTION

In his seminal paper of 1940 on activated-rate processes [1], Kramers considered the escape rate of a one dimensional particle with coordinate q trapped in a metastable potential well of a potential function $V(q)$. The dynamics of the particle is described by a Langevin equation in which it experiences a frictional force characterized by a damping constant γ and an external Gaussian Markoffian random force. The particle can escape from the well by crossing a potential barrier. When the damping is weak, Kramers showed that the escape rate is limited by the rate of transfer of energy to the particle from the heat bath and so is proportional to the damping. When the damping is moderate or strong, the process is limited by the spatial rate of passage of the particle across the barrier [2,3] In this paper we will consider the dynamics in this so called spatial diffusion limit.

Kramers's one dimensional problem may be generalized by introducing memory friction. Instead of the Langevin equation of motion, one may consider a generalized Langevin equation (GLE) in which the friction function is no longer Markoffian. The effect of memory friction on activated-rate processes has been studied extensively during the past decade [3,4]. Grote and Hynes [5] generalized Kramers's expression for the rate in the spatial diffusion limit. They pointed out that the rate for spatial diffusion across a barrier is a function of frequency dependent friction and is determined by the component of the friction at the barrier frequency rather than the static friction as in Kramers' original theory.

A further refinement of Kramers theory may be obtained by introducing also a space dependent friction. The equation of motion, as derived first by Lindenberg and co-workers [6,7] is substantially more complex looking than the GLE. Nevertheless, Carmeli and Nitzan [8] derived an expression for the rate in the energy diffusion limited regime in the presence of space dependent friction.

This sums up the state of affairs as of the middle of the 1980s. The dominant theoretical approach was based primarily on a steepest descent estimate for the rate, which is identical to considering only the dynamics of the parabolic vicinity of the potential barrier. During the past few years it has become evident that the Kramers-Grote-Hynes theory may be insufficient. One failing is related to memory friction. For long memory, there will be an intermediate range of damping values, for which the motion across the barrier occurs on a time scale which is similar to the memory time. When this occurs, and the nonlinearity of the potential is not negligibly small, the particle will remember the nonlinearity and one may observe rate suppression [9.10]. The magnitude of the nonlinearity is controlled by the temperature in terms of the reduced barrier height $\frac{V^{\ddagger}}{k_B T}$.

A different mechanism which may lead to deviations from the parabolic barrier limit has to do with spatial dependent friction. If the friction is much larger away from the barrier then one should expect that the effective friction is larger than used in the standard theory and the rate would be suppressed. In the presence of memory friction the effect may be stronger, since the particle will remember the larger damping strength exerted upon it as it moves along the barrier. Deviations from the Kramers-Grote-Hynes limit induced by memory and space dependent friction have been recently observed in numerical simulations by Voth and co-workers [11,12].

In recent years we have introduced the variational-transition-state theory (VTST) approach to activated-rate processes in the spatial diffusion limit [13–15]. Instead of dealing with a stochastic differential equation, one may recast the GLE in terms of a Hamiltonian in which the system is coupled to a harmonic bath [16,17]. The dynamics of the GLE may be represented as the continuum limit of the Hamiltonian dynamics.

Transition-state theory (TST) [18,19], which is applicable to Hamiltonian systems, provides an upper bound [20] to the decay rate by considering the unidirectional flux across a dividing surface between "reactants" and "products." TST is exact if the particle does not recross the dividing surface. Otherwise, it gives an upper bound to the rate, since any recrossing is counted as a reactive event. By varying the dividing surface one may find a

*Permanent address: Karpov Institute of Physical Chemistry, ul. Obukha 10, 103064 Moscow K-64, Russia.

minimal upper bound, hence the name variational transition state theory.

In general, especially for a system as complicated as the Hamiltonian equivalent of the GLE, one might expect that the variational procedure is rather cumbersome and difficult. We have shown though that substantial progress may be achieved by optimizing a planar dividing surface in the full configuration space of the system and the bath [21,22]. For high barriers, such an optimization reduces to the Kramers-Grote-Hynes theory. In the presence of nonlinearity, optimized planar dividing surfaces account correctly for the effects of memory [10] and space dependent friction [23]

Thus far though, most applications of the optimized planar dividing surface VTST were restricted to symmetric potentials. The asymmetric case is in fact much more interesting since here one will also find a shift of the dividing surface away from the barrier top [22]. The main obstacle in dealing with asymmetric systems may be understood by considering the extreme asymmetric cubic potential. In this case, strictly speaking, any planar dividing surface which is not perpendicular to the particle coordinate q will give an infinite upper bound because of nonphysical contributions to the flux from very large values of q. This raises the question of whether it is still possible to retain the power of the optimized planar dividing surface approach for the class of metastable potentials which is unbounded from below. The main purpose of the present paper is to further extend the optimal planar dividing surface approach to this general class of potentials. This will also allow us to justify our previous use [22,24] of a perturbation expansion of the rate expression in terms of the inverse reduced barrier height although in principle, the expansion may be divergent.

The extension is based on the observation that if the planar dividing surface is perpendicular to the particle coordinate then the divergence is removed. A straightforward extension of the optimized planar dividing surface is to allow for a bent dividing surface which is composed of two planes. For almost all values of the particle coordinate one uses the usual planar dividing surface. However, when the particle coordinate becomes larger than some value denoted as q_0, one bends the surface so that it becomes perpendicular to q. This added "kink parameter" becomes a variational parameter and one can uniquely determine the optimal place at which the kink should be introduced.

In Sec. II we review briefly the optimized planar dividing surface approach and introduce the bent dividing surface. Practical application to cubic and asymmetric quartic potentials is presented in Secs. III and IV. We end with a discussion of the practical implications when dealing with more complicated systems.

II. OPTIMAL BENT PLANAR DIVIDING SURFACES

A. Planar dividing surfaces

The GLE for a one dimensional system is of the form

$$\ddot{q} + \frac{dV(q)}{dq} + \int_0^t d\tau\, \gamma(t-\tau)\dot{q}(\tau) = \xi(t). \tag{2.1}$$

Here, q is the (mass weighted) system coordinate and $V(q)$ is the system potential. The Gaussian random force $\xi(t)$ is related to the friction kernel $\gamma(t)$ through the second fluctuation dissipation theorem: $\langle \xi(t)\xi(0)\rangle = \frac{1}{\beta}\gamma(t)$ and we use the notation $\beta \equiv \frac{1}{k_B T}$ throughout this paper.

The dynamics of the GLE (2.1) is equivalent to the dynamics of the system bath Hamiltonian [16, 17]

$$H = \frac{p_q^2}{2} + V(q) + \sum_j \frac{1}{2}\left[p_{x_j}^2 + \left(\omega_j x_j - \frac{c_j q}{\omega_j}\right)^2\right], \tag{2.2}$$

where the system coordinate q is coupled bilinearly to a bath of harmonic oscillators with frequencies ω_j. The summation is in principle over an infinite set of bath oscillators which tends towards a continuum. The bath coordinates x_j are mass weighted. By explicit solution for the time dependence of each of the bath coordinates, one can show that Hamilton's equations of motion for the system coordinate q reduce to the GLE (2.1), with the identification that

$$\gamma(t) = \sum_j \frac{c_j^2}{\omega_j^2}\cos(\omega_j t). \tag{2.3}$$

Transition state theory gives the escape rate as a ratio of the equilibrium unidirectional flux to the equilibrium population of reactants [18, 19, 25]:

$$\Gamma = \frac{\int dp_q dq \prod_j dp_{x_j} dx_j \delta(f)(\nabla f\cdot\mathbf{p})\theta(\nabla f\cdot\mathbf{p})e^{-\beta H}}{\int dp_q dq \prod_j dp_{x_j} dx_j \theta(-f)e^{-\beta H}}. \tag{2.4}$$

The Dirac delta function $\delta(f)$ localizes the integration onto the dividing surface $f = 0$. The gradient of the surface (∇f) is in the full phase space, $\mathbf{p}$ is the generalized velocity vector in phase space with components $\dot{q}, \dot{p}_q[(\dot{x}_j, \dot{p}_{x_j}), j = 1, ..., N]$ and $\theta(y)$ is the unit step function which chooses the flux in one direction only. The term $\nabla f \cdot \mathbf{p}$ is proportional to the velocity perpendicular to the dividing surface. The TST expression is an *upper bound* for the rate. VTST is obtained by varying the dividing surface f looking for that dividing surface which gives the least upper bound.

The choice for the transition state implicit in Kramers's paper is the barrier top ($q = 0$) of the potential $V(q)$. In this case the dividing surface takes the form $f = q = 0$ and the rate expression (2.4) reduces to the well known one dimensional result:

$$\Gamma_{1D} = (2\pi\beta)^{-\frac{1}{2}} \frac{e^{-\beta V(0)}}{\int dq \theta(-q)e^{-\beta V(q)}} \simeq \frac{\omega_a}{2\pi} e^{-\beta V^\ddagger}, \tag{2.5}$$

where ω_a is the frequency at the bottom of the well.

The Kramers-Grote-Hynes expression for the rate may be derived from the TST formulation by noting that for a purely parabolic barrier $[V(q) = V(0) - \frac{1}{2}\omega^{\ddagger 2} q^2]$ the Hamiltonian (2.2) is a bilinear form which may be diagonalized using a normal mode transformation [13]. In the diagonal form, one finds one unstable mode, denoted ρ, with associated barrier frequency, denoted $\lambda_\infty^\ddagger$ and N stable modes. The ∞ subscript will serve to remind us

that this is the solution for the purely parabolic barrier, or equivalently for an infinite reduced barrier height. The normal mode barrier frequency ($\lambda_\infty^\ddagger$) is the solution of the equation

$$\omega^{\ddagger^2} = \lambda_\infty^{\ddagger^2}\Big(1 + \frac{\hat{\gamma}(\lambda_\infty^\ddagger)}{\lambda_\infty^\ddagger}\Big) , \tag{2.6}$$

where $\hat{\gamma}(s)$ denotes the Laplace transform of the friction kernel with frequency s. The rate may now be obtained by choosing the dividing surface $f = \rho = 0$. The result is the usual Kramers-Grote-Hynes result [1,5] for the spatial diffusion limit:

$$\Gamma_\infty = \frac{\lambda_\infty^\ddagger}{\omega^\ddagger}\Gamma_{1D}. \tag{2.7}$$

Note that the Kramers-Grote-Hynes solution has been obtained by replacing the one dimensional dividing surface $f = q = 0$ by a dividing surface in the full space of system and bath, $f = \rho = u_{00}q + \sum_j u_{0j}x_j = 0$, where the u_{ij}'s are elements of the orthogonal normal mode transformation matrix. To obtain a generalization of this approach, in the presence of a finite reduced barrier height ($\beta V^\ddagger$) we pose the following question: *what is the optimal* **planar** *dividing surface?* The most general planar dividing surface (in configuration space) may be written as

$$f = a_0 q + \sum_j a_j x_j - \rho_0 = 0 , \tag{2.8}$$

where ρ_0 denotes the distance of the dividing surface from the origin and $a_0, a_j, j = 1, ..., N$ are the components of the unit vector perpendicular to the dividing surface. A generalization of the Kramers-Grote-Hynes theory, is obtained by minimizing the TST expression for the rate with respect to the coefficients $a_0, a_j, j = 1, ..., N$ and the shift ρ_0. The details are given explicitly in Ref. [22]; here we summarize the results needed to apply the theory.

The optimized estimate for the rate is

$$P_0 \equiv \frac{\Gamma}{\Gamma_{1D}} = \Big(\frac{\beta A^2}{2\pi}\Big)^{\frac{1}{2}} \int_{-\infty}^{\infty} dq \exp[-\beta V_{\text{eff}}(q, \rho_0)] , \tag{2.9}$$

where the effective potential has the form

$$V_{\text{eff}}(q, \rho) \equiv \tfrac{1}{2}A^2(Cq - \rho)^2 + V(q) - V(0) . \tag{2.10}$$

The optimized effective frequency A and coupling constant C are expressed in terms of the temperature dependent effective barrier frequency $\lambda^\ddagger$ through the following relations:

$$A^2 = \left[\sum_j \frac{a_j^2}{\omega_j^2}\right]^{-1} = \frac{\lambda^{\ddagger^2}}{a_0 C - 1} , \tag{2.11}$$

$$C = a_0 + \sum_j \frac{a_j c_j}{\omega_j^2} = a_0\Big(1 + \frac{\hat{\gamma}(\lambda^\ddagger)}{\lambda^\ddagger}\Big) . \tag{2.12}$$

In this last expression the projection a_0 of the system coordinate q onto the direction perpendicular to the dividing surface may also be expressed in terms of the barrier frequency $\lambda^\ddagger$ by using the normalization condition for the transformation coefficients:

$$a_0^2 = 1 - \sum_j a_j^2 = \Big[1 + \frac{1}{2}\Big(\frac{\hat{\gamma}(\lambda^\ddagger)}{\lambda^\ddagger} + \frac{\partial\hat{\gamma}(s)}{\partial s}\Big|_{s=\lambda^\ddagger}\Big)\Big]^{-1} . \tag{2.13}$$

The effective barrier frequency ($\lambda^\ddagger$) is now determined by a generalization of the Kramers-Grote-Hynes equation (2.6):

$$A^2C^2 - \frac{1}{\beta\langle(q - \langle q\rangle)^2\rangle} = \lambda^{\ddagger^2}\Big(1 + \frac{\hat{\gamma}(\lambda^\ddagger)}{\lambda^\ddagger}\Big) . \tag{2.14}$$

where we have used the notation

$$\langle q^n\rangle \equiv \frac{P_n}{P_0} , \tag{2.15}$$

$$P_n \equiv \Big(\frac{\beta A^2}{2\pi}\Big)^{\frac{1}{2}} \int_{-\infty}^{\infty} dq q^n \exp[-\beta[V_{\text{eff}}(q, \rho_0)] . \tag{2.16}$$

Finally the shift parameter is determined by the equation

$$\rho_0 = C\langle q\rangle \tag{2.17}$$

from which it is clear that for a symmetric potential a solution for the shift parameter is $\rho_0 = 0$.

Equation (2.14) for the barrier frequency $\lambda^\ddagger$ and (2.17) for the shift ρ_0 must be solved simultaneously. Then, one can find the parameters A and C necessary to evaluate the optimized rate. In practice, instead of solving the transcendental equations for the optimized barrier frequency (2.14) and the shift (2.17) one may minimize the expression for the transmission probability (2.9) directly. Since the dependence of the parameters A and C on the barrier frequency $\lambda^\ddagger$ is known [cf. Eqs. (2.11)–(2.13)], one may think of the transmission probability P_0 given in Eq. (2.9) as a function of the two independent variables $\lambda^\ddagger, \rho_0$ and minimize the function numerically. For a symmetric potential this procedure is even simpler, since there is no shift ($\rho_0 = 0$). The transmission probability is a function of one variable only ($\lambda^\ddagger$), and one need only find its minimum.

B. Bent planar dividing surfaces

Inspection of the result for the transmission coefficient through a planar dividing surface [Eqs. (2.9),(2.10)] shows immediately that for a cubic potential the transmission coefficient will diverge. This divergence is not restricted to cubic potentials, it will occur in principle, for any potential which does not go to $+\infty$ when $q \to \pm\infty$. On the other hand, the flux through the dividing surface will not diverge for any dividing surface of the form $f = q - q_0$. To circumvent the divergence we will use a bent planar dividing surface.

To introduce the kink we define two perpendicular coordinates

$$\rho \equiv a_0 q + \sum_j a_j x_j \ , \tag{2.18}$$

$$\sigma \equiv a_I q - \frac{a_0}{a_I} \sum_j a_j x_j \ , \tag{2.19}$$

such that

$$q = a_0 \rho + a_I \sigma, \tag{2.20}$$

where we have used the shorthand notation

$$a_I^2 \equiv 1 - a_0^2. \tag{2.21}$$

At this point, the effective potential $V_{\text{eff}}(q, \rho_0)$ [cf. Eq. (2.10)] may be thought of as a function of the two independent variables ρ and σ. The bent dividing surface is then defined in the (ρ, σ) plane and consists of two parts. Without loss of generality, we assume that the potential $V(q)$ goes to $\pm\infty$ as $q \to \mp\infty$, respectively. For $q \leq q_0$, where q_0 denotes the "kink" point, the dividing surface takes the usual form $f = \rho - \rho_0$ [cf. Eq. (2.8)]. The kink point q_0 defines a point ρ_0, σ_0 in the (ρ, σ) plane, such that the bent dividing surface has the form (see Fig. 1 below)

$$f = \begin{cases} \rho - \rho_0, & \text{if } \sigma \leq \sigma_0 \\ q - q_0, & \text{if } \sigma \geq \sigma_0 \ , \end{cases} \tag{2.22}$$

where

$$q_0 = a_0 \rho_0 + a_I \sigma_0. \tag{2.23}$$

Insertion of this form for the dividing surface into the TST rate expression (2.4) and normalizing by the one dimensional rate [Eq. (2.5)] gives a modified expression for the transmission coefficient (see Appendix A for the detailed derivation):

$$P_0 = \left(\frac{\beta A^2}{2\pi}\right)^{\frac{1}{2}} \left(\int_{-\infty}^{q_0} dq \exp[-\beta V_{eff}(q, \rho_0)] + \int_{-\infty}^{\rho_0} d\rho \exp[-\beta V_{\text{eff}}(q_0, \rho)] \right) . \tag{2.24}$$

The two terms in this expression correspond to two contributions to the outgoing flux. The first term gives the flux in the ρ direction. This is the usual contribution to the flux obtained from the planar dividing surface $f = \rho - \rho_0$ in the region $\sigma \leq \sigma_0$. The second term gives the contribution in the q direction and comes from that part of the dividing surface in which $f = q - q_0$ $(\sigma \geq \sigma_0)$; see Fig. 1 below. The dependence of the frequency A and coupling constant C on the transformation coefficients remains as for the usual planar dividing surface; see the first equalities in Eqs. (2.11) and (2.12).

Equation (2.24) is the central formal result of this paper. One notes that at this point the divergence has been removed. The contribution of the second term in the outgoing flux due to the kink is of order $e^{-\beta V_{eff}(q_0, \rho_0)}$. If the kink is not too close to the barrier top this will give an exponentially small correction. It is thus not surprising that a perturbation expansion for the rate which is based on a planar dividing surface will give a good estimate, even though strictly speaking, the expansion is divergent unless one introduces the kink. The leading term in an expansion in terms of the inverse barrier height $(\frac{1}{\beta V^\ddagger})$ will remain the same, whether one does or does not in-

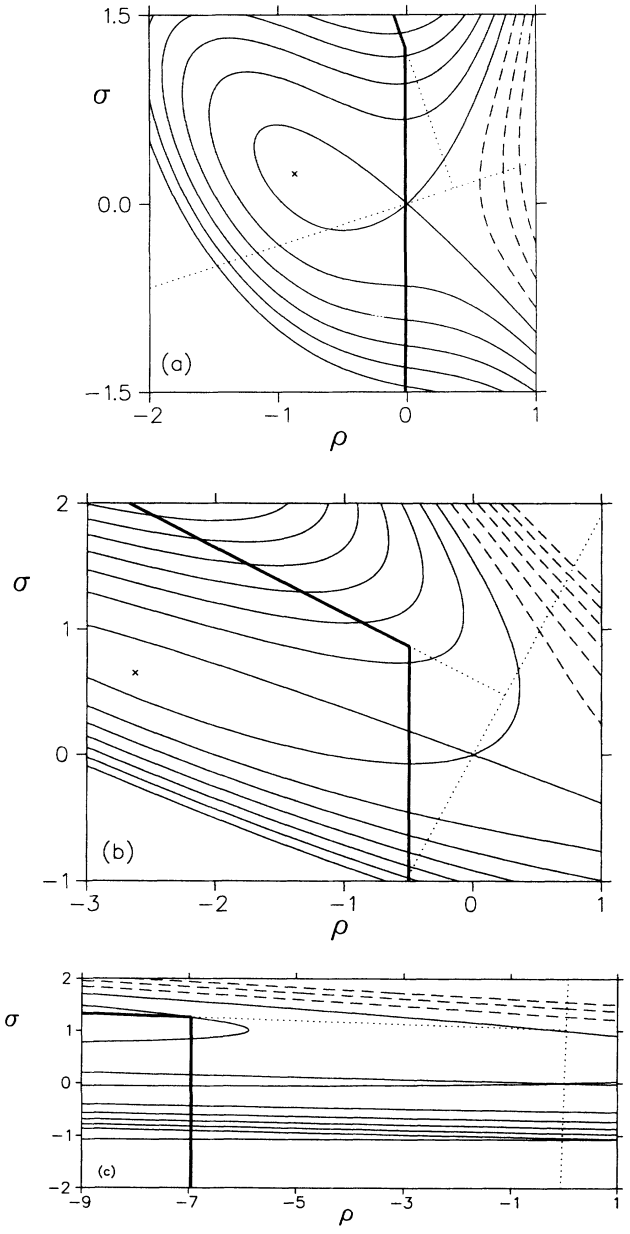

FIG. 1. Optimized bent dividing surfaces for the cubic potential and Ohmic friction. The reduced barrier height is $\beta V^\ddagger = 1$. Solid lines are equipotential lines at the positive reduced energies (in units of $\beta V^\ddagger$) 0, 3, 6, 9, ...; dashed lines are negative energy contours at $-3, -6, \ldots$. The heavy solid lines are the optimized dividing surfaces. The dotted line that goes through the origin ($\rho = \sigma = 0$) is the q axis and the dotted line perpendicular to it crosses the q axis at the kink point $q = q_0$. The cross denotes the location of the well whose reduced energy is -1. Panels (a)–(c) are for $\chi = 1.1, 1.75, 1.999$, respectively, corresponding to the reduced damping values $\alpha = 0.1, 1.1, 22.3$, respectively. The three cases cover the weak, intermediate, and strong damping cases.

troduce the kink in the dividing surface to remove the divergence.

Optimizing the transmission coefficient with respect to the a_j's leads to the same equations as before, that is the frequency A, the coupling constant C and the coefficient a_0 are all expressed in terms of the Laplace transform of the time dependent friction and the effective barrier frequency $\lambda^\ddagger$ as in the second equalities of Eqs. (2.11)–(2.13). At this point, the transmission coefficient is a function of three variables $P_0 = P_0(\lambda^\ddagger, \rho_0, q_0)$.

It is possible to simplify the computation by explicit variation of the transmission probability with respect to the kink parameter. One finds (after an integration by parts)

$$\frac{\partial P_0}{\partial q_0} = 1 - C - \beta \frac{dV(q)}{dq}\bigg|_{q=q_0} \cdot \times \int_0^\infty dy\, e^{-\beta A^2[(Cq_0-\rho_0)y+\frac{1}{2}y^2]} = 0 \,. \tag{2.25}$$

In this equation one may treat the variable $Cq_0-\rho_0$ which appears in the integrand as an independent parameter instead of ρ_0, such that one is left with an equation for the kink parameter q_0 in terms of the other variables. This is especially useful for a cubic potential for which the equation is quadratic and thus easy to solve (cf. Sec. III). One then remains with a minimization with respect to two variables, which may be carried out numerically.

It is also possible to obtain an asymptotic ($C >> 1$) solution to Eq. (2.25) for the kink point q_0. The leading order term in such an expansion is obtained by ignoring the term $\frac{1}{2}y^2$ in the exponent of the integrand in Eq. (2.25). The solution for the kink point obtained in this way is identical to finding a maximum of the effective potential $V_{\text{eff}}(q, \rho_0)$; cf. Eq. (2.10). From the structure of the potential $V(q)$ one knows that $V_{\text{eff}}(q) \to \pm\infty$ as $q \to \mp\infty$, respectively. One also expects that the effective potential will have a minimum at some value of q, which will be separated from the asymptotic limit of $-\infty$ by a maximum. If the maximum and minimum are well separated, then the asymptotic estimate for q_0 as the maximum will usually be very good, and in addition, the kink term will contribute only an exponentially small term to the flux.

In summary, we have shown that introduction of a bent dividing surface will remove in principle any divergence which may result from a potential which does not become infinitely high as $q \to \pm\infty$. All that happens is that one must introduce an additional variational parameter q_0 which is the location of the kink in the dividing surface. In the next section we will consider the example of the cubic potential in some detail.

III. APPLICATION TO A CUBIC POTENTIAL

In this section we demonstrate a bent planar dividing surface for the case of Ohmic friction;

$$\gamma(t) = 2\gamma\delta(t) \tag{3.1}$$

and the cubic potential:

$$V(q) = V(0) - \frac{1}{2}\omega^{\ddagger 2} q^2\left(1 + \frac{q}{q_1}\right) , \tag{3.2}$$

where q_1 is the characteristic length. The well bottom is located at $q = -\frac{2}{3}q_1$ and the barrier height is $V^\ddagger = \frac{2}{27}\omega^{\ddagger 2} q_1^2$.

As already mentioned in the preceding section, for the cubic potential it is convenient to consider the variables $\lambda^\ddagger, \rho_1 \equiv Cq_0 - \rho_0$ and q_0 as the independent variables, instead of $\lambda^\ddagger, \rho_0, q_0$. This allows one to use Eq. (2.25) to determine q_0 as a function of $\lambda^\ddagger$ and ρ_1 so that $q_0 = q_0(\lambda^\ddagger, \rho_1)$. Then ρ_0 may be extracted from the definition of the variable ρ_1, so that at this point, the transmission coefficient is also a function of only two variables $P_0 = P_0(\lambda^\ddagger, \rho_1)$. The remaining minimization is done numerically.

We have studied in detail the case of a low barrier $\beta V^\ddagger = 1$, since this example has also been studied previously in Refs. [10, 26]. In the case of Ohmic friction [$\gamma(t) = 2\gamma\delta(t)$], Eqs. (2.11)–(2.13) take the form

$$A^2 = \frac{2\lambda^{\ddagger 3}}{\gamma}\left[1 + \frac{\gamma}{2\lambda^\ddagger}\right] ; \tag{3.3}$$

$$C = \left(1 + \frac{\gamma}{2\lambda^\ddagger}\right)^{-\frac{1}{2}}\left[1 + \frac{\gamma}{\lambda^\ddagger}\right] ; \tag{3.4}$$

$$a_0^2 = \left[1 + \frac{\gamma}{2\lambda^\ddagger}\right]^{-1} . \tag{3.5}$$

To simplify, we use the dimensionless variable $\alpha \equiv \frac{\gamma}{2\omega^\ddagger}$ and the "nonlinearity parameter" (cf. Ref. [9])

$$\chi \equiv 1 + \frac{\alpha}{(1+\alpha^2)^{\frac{1}{2}}}, \tag{3.6}$$

which varies in the range $(1, 2)$ as the dimensionless friction constant α varies in the range $(0, \infty)$.

Optimal bent planar dividing surfaces are shown in Fig. 1 for three values of α. The contours are the equipotential lines of the effective potential $V_{\text{eff}}(q = a_0\rho + a_I\sigma, \rho_0)$; cf. Eq. (2.10). The three panels in Fig. 1 are for the values $\chi = 1.1, 1.75$, and 1.999, which correspond to $\alpha = 0.1, 1.1$, and 22.3, respectively. These are typical of weak damping, intermediate and strong damping, respectively.

Figure 1 demonstrates three properties of the optimized dividing surface. As the damping varies from weak to strong, one finds that (1) the angle between the ρ and q axes increases from 0 to $\frac{\pi}{2}$; (2) the location of the kink point q_0 varies from $q_0 = \frac{q_1}{3}$ for $\gamma = 0$ to $q_0 = \frac{1}{3}[1+\sqrt{7}]q_1$ as $\gamma \to \infty$, as shown analytically in Appendix B; and (3) the shift ρ_0 increases its absolute value with increasing damping. The optimal dividing surface moves from the barrier top ($\rho_0 = 0$, for $\gamma = 0$) towards the direction of the well of the cubic potential. This qualitative result is in agreement with the asymptotic estimates for the shift presented in Ref. [22].

It is of interest to compare the transmission coefficient obtained from optimization of the bent planar dividing surface with previous estimates for the rates. These include (a) Kramers' expression [1]

$$P_{\rm Kr} = (1+\alpha^2)^{\frac{1}{2}} - \alpha \ , \tag{3.7}$$

which is based on a steepest descent estimate for the rate at the barrier top, valid in principle only for $\beta V^{\ddagger} >> 1$; and (b) the curved dividing surface canonical VTST of Ref. [9], in which one uses the normal modes of the parabolic barrier Hamiltonian to construct an effective free energy Hamiltonian in two degrees of freedom. The optimal curved dividing surface is found as an infinite period orbit dividing surface of the effective Hamiltonian. The comparison is given is Table I. The striking result is the closeness of all three methods. It is evident, that even though the barrier is low, in the case of Ohmic friction, the simple steepest descent estimate of Kramers suffices for numerical purposes.

It is also evident that the two variational TST approaches are very similar. Here we note though that the present approach could be further improved. One can use the optimized bent planar dividing surface to construct the effective two-degree-of-freedom Hamiltonian

$$H_{\rm 2D} = \tfrac{1}{2}(p_\rho^2 + p_\sigma^2) + V_{\rm eff}(q = a_0\rho + a_1\sigma, \rho_0) \ , \tag{3.8}$$

where the effective potential $V_{\rm eff}$ is the same as given in Eq. (2.10). The improved estimate is then obtained by finding the infinite period orbit dividing surface on this effective Hamiltonian. However, for the case of Ohmic friction studied in this paper, the added effort is not worthwhile.

IV. THE ASYMMETRIC QUARTIC POTENTIAL

The cubic potential considered in the preceeding section is an extreme case of asymmetry between the reactant and product wells. The usual more realistic case of a finite energy difference between reactants and products is better represented by the asymmetric quartic potential

$$V(q) = -\frac{1}{2}\omega^{\ddagger 2} q^2 \Big[1 + \frac{2}{3}\frac{q_+ - q_-}{q_+ q_-} q - \frac{1}{2}(q_+ q_-)^{-1} q^2\Big] \ . \tag{4.1}$$

In this form, the potential barrier is at the origin ($q = 0$). The left well has a minimum at the point $-q_-$, while the right well has a minimum at q_+ and $q_-, q_+ > 0$. The potential is drawn schematically in Fig. 2. The well depths may be denoted V_-, V_+ for the left and right wells, respectively, and one finds that

$$V_+ = V_- q_{\rm as}^3 \frac{2 + q_{\rm as}}{1 + 2q_{\rm as}} \ , \tag{4.2}$$

where the ratio $q_{\rm as} = \frac{q_+}{q_-}$ measures the asymmetry of the potential. When $q_{\rm as} = 1$ the potential is symmetric, when $q_{\rm as} \to \infty$ one recovers the cubic potential of Sec. III. Without loss of generality, we will only consider cases for which $q_{\rm as} \geq 1$ such that the right well is deeper than the left well and we are estimating the escape rate of the particle from left to right.

For a purely planar dividing surface, the cubic potential gives a divergent upper bound, but the quartic potential, because of the q^4 term will always give a finite result. The introduction of a kink into the planar dividing surface becomes important for the quartic potential only if it leads to an essential improvement over the planar dividing surface.

In Fig. 3, we compare the results for the quartic potential which are obtained by using a planar dividing surface, with those obtained in the cubic case using a bent dividing surface. The reduced barrier height is $\beta V_- = 5$ and the asymmetry in the quartic potential is $q_{\rm as} = 10$. This corresponds to $\beta V_+ \simeq 3 \times 10^3$. As may be seen from the figure, for any value of the damping, the introduction of a kink in the dividing surface will not lead to an essential improvement in the estimate for the transmission probability. It is of interest to note though that both the shift and the optimized barrier frequency are somewhat different, however, the differences almost disappear by

TABLE I. Transmission probability for the cubic potential.

χ	α	$\frac{\Gamma_{bpl}}{\Gamma_{\rm Kr}}$ [a,b]	$\frac{\Gamma_{bpl}}{\Gamma_{\rm Fe}}$ [c]	$\frac{j_q}{j_\rho}$ [d,e]
1.1	0.1	0.999	1.001	1×10^{-6}
1.75	1.1	0.967	1.003	0.001445
1.999	22.3	0.996	0.993	0.00000

[a] Γ_{bpl} is the estimate based on the optimal bent planar dividing surface, Eq. (2.24).
[b] $\Gamma_{\rm Kr}$ is the Kramers estimate for the rate.
[c] $\Gamma_{\rm FP}$ is the estimate based on the curved dividing surfaces of Ref. [9].
[d] j_q is the flux through the part of the bent dividing surface for which $f = q - q_0$.
[e] j_ρ is the flux through the part of the bent dividing surface for which $f = \rho - \rho_0$.

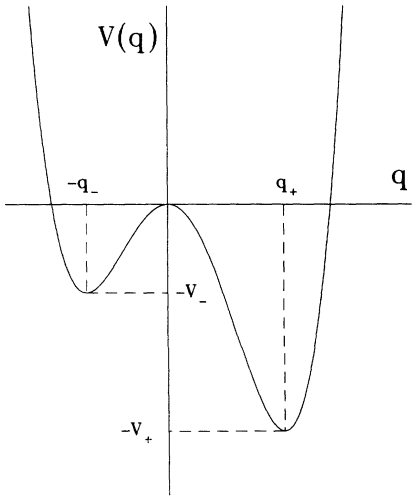

FIG. 2. Schematic drawing of the asymmetric quartic potential [cf. Eq. 4.1].

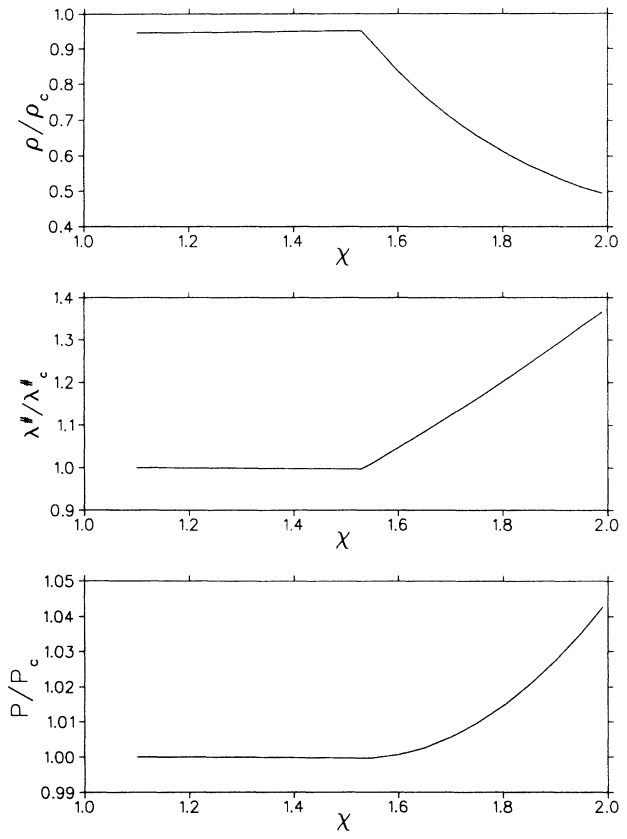

FIG. 3. Optimized results for the asymmetric quartic potential. The barrier height is $\beta V_- = 5$ and the right well is much deeper than the left well ($V_+/V_- \simeq 600$). Results for the quartic potential, based on an optimized planar dividing surface, are presented as ratios to optimized results for a cubic potential with the same barrier height. Panels (a)–(c) correspond to the optimized shift, barrier frequency, and transmission probability, respectively.

the time one considers the probability. From a practical point of view, we conclude that, for most purposes, when considering a quartic asymmetric potential or a potential similar to it, one can limit oneself to the easier problem of a planar dividing surface.

V. DISCUSSION

In this paper we have explored the application of variational-transition-state theory to extremely asymmetric activated-rate processes. From the formal point of view, we have shown that one can generalize the class of optimized planar dividing surfaces by introducing a kink, which leads to good estimates for the rate even in the case of a purely cubic potential. Introduction of the kink shows explicitly why one can use a steepest descent expansion for the shift, optimized barrier frequency and transmission coefficient as in Ref. [22] even though strictly speaking the planar dividing surface gives an infinite upper bound. We have seen that the kink will usually introduce corrections which are exponentially small, which are justifiably neglected in the steepest descent expansion which considers much larger terms which are of the order of $(\beta V^{\ddagger})^{-n}$.

From the practical point of view, we have demonstrated explicitly that in asymmetric cases, there may be a substantial shift of the optimized planar dividing surface away from the top of the barrier. The magnitude of the shift depends on the (reduced) barrier height and will become less important as the barrier height is increased. Qualitatively we have seen that there isn't much difference between a cubic potential and a highly asymmetric quartic potential and moreover, there is no practical need to introduce a kink in the quartic case. We expect the same to remain true also when dealing with memory friction.

This paper was limited to one dimensional activated-rate processes. There is however no practical problem of generalizing the kink in the dividing surface to the multidimensional case. It is also straightforward to introduce the bent dividing surface in the presence of space dependent friction. However, one may expect that for most realistic systems this added complication is not necessary. Except for cases with very low barriers or extreme asymmetry (such as the cubic potential) the planar dividing surface should suffice.

ACKNOWLEDGMENTS

This work has been supported by grants from the Minerva Foundation, the Israeli Ministry for Absorption of Immigrant Scientists, and the Einstein center at the Department of Physics of the Weizmann Institute of Science.

APPENDIX A: DERIVATION OF EQ. (2.24)

The transmission coefficient [Eq. (2.9)] is defined as the ratio of the rate constant Γ to the one dimensional rate Γ_{1D} and so may be written in the form [cf. Eqs. (2.4), (2.5)]:

$$P_0 = \frac{\int dp_q dq \prod_j dp_{x_j} dx_j \delta(f)(\nabla f \cdot \mathbf{p})\theta(\nabla f \cdot \mathbf{p}) e^{-\beta H}}{\int dp_q dq \prod_j dp_{x_j} dx_j \delta(f_0)(\nabla f_0 \cdot \mathbf{p})\theta(\nabla f_0 \cdot \mathbf{p}) e^{-\beta H}} \tag{A1}$$

where the Hamiltonian is the system bath Hamiltonian given in Eq. (2.2). The dividing surface f_0 is the plane perpendicular to the system coordinate, which goes through the saddle point $q = x_1 =, \ldots, x_n = 0$, that is $f_0 = q$. The denominator in Eq. (A1) is therefore $\beta^{-1} \prod_j \frac{2\pi}{\beta\omega_j}$. The transmission coefficient now takes the form

$$P_0 = \beta \Big(\prod_j \frac{\beta\omega_j}{2\pi} \Big) \int dp_q dq \times \prod_j dp_{x_j} dx_j \delta(f)(\nabla f \cdot \mathbf{p})\theta(\nabla f \cdot \mathbf{p}) e^{-\beta H} . \tag{A2}$$

Using the definitions of the coordinates ρ and σ as given in Eqs. (2.18) and (2.19), defining the corresponding momenta

$$p_\rho \equiv a_0 p_q + \sum_j a_j p_{x_j} \ , \tag{A3}$$

$$p_\sigma \equiv a_I p_q - \frac{a_0}{a_I} \sum_j a_j p_{x_j} \ , \tag{A4}$$

and applying the identity

$$1 = \int_{-\infty}^{\infty} \delta(z - z_0) dz, \tag{A5}$$

one may rewrite Eq. (A2) as

$$P_0 = \beta \Big(\prod_j \frac{\beta\omega_j}{2\pi} \Big) \int dp_\rho d\rho dp_\sigma d\sigma \delta(f) (\nabla f \cdot \mathbf{p}) \theta(\nabla f \cdot \mathbf{p}) e^{-\beta V(a_0\rho + a_I\sigma)} J(p_\rho, \rho, p_\sigma, \sigma), \tag{A6}$$

where

$$\begin{aligned} J(p_\rho, \rho, p_\sigma, \sigma) = & \int dp_q dq \prod_j dp_{x_j} dx_j e^{-\beta[H - V(q)]} \\ & \times \delta\Big(\rho - (a_0 q + \sum_j a_j x_j) \Big) \delta\Big(\sigma - (a_I q - \frac{a_0}{a_I} \sum_j a_j x_j) \Big) \\ & \times \delta\Big(p_\rho - (a_0 p_q + \sum_j a_j p_{x_j}) \Big) \delta\Big(p_\sigma - (a_I p_q - \frac{a_0}{a_I} \sum_j a_j p_{x_j}) \Big) \\ = & \frac{\beta}{2\pi} \Big(\prod_j \frac{2\pi}{\beta\omega_j} \Big) a_I A e^{-\frac{\beta}{2}\left(p_\rho^2 + p_\sigma^2 + A^2[(a_0 C - 1)\rho + a_I C \sigma]^2\right)}. \end{aligned} \tag{A7}$$

The frequency A and coupling constant C appearing in the integrand are the same as defined in Eqs. (2.11) and (2.12), respectively. As a result the transmission coefficient is simplified to

$$P_0 = \frac{\beta^2}{2\pi} a_I A \int dp_\rho d\rho \, dp_\sigma d\sigma \, \delta(f) (\nabla f \cdot \mathbf{p}) \theta(\nabla f \cdot \mathbf{p}) e^{-\beta \tilde{H}} \tag{A8}$$

where

$$\begin{aligned} \tilde{H} \equiv & \tfrac{1}{2}[p_\rho^2 + p_\sigma^2 + V(a_0\rho + a_I\sigma)] \\ & + \tfrac{1}{2} A^2 [C(a_0\rho + a_I\sigma) - \rho]^2 \ , \end{aligned} \tag{A9}$$

The bent planar dividing surface has been defined in Eq. (2.22). The momentum perpendicular to the dividing surface is

$$(\nabla f \cdot \mathbf{p}) = \begin{cases} p_\rho, & \text{if } \sigma \le \sigma_0 \\ a_0 p_\rho + a_I p_\sigma, & \text{if } \sigma \ge \sigma_0 \end{cases} . \tag{A10}$$

Introduction of Eqs. (2.22) and (A10) in Eq. (A8) leads after several integrations to Eq. (2.24) which is the main result of this paper.

APPENDIX B: ANALYTIC ESTIMATES FOR THE LOCATION OF THE KINK POINT

For Ohmic friction, we consider the two limits $\gamma \to 0$ and $\gamma \to \infty$ separately. When $\gamma \to 0$, the barrier frequency is $\lambda^\ddagger \simeq \omega^\ddagger$, the coupling constant $C \simeq 1 + \frac{3}{2\alpha}$ and the frequency A is $A^2 \simeq \frac{\omega^{\ddagger 2}}{\alpha}$. In this case, the integral in Eq. (2.25) may be estimated as $\frac{1}{\beta A^2 q_0}$ and Eq. (2.25) may be written as

$$A^2(C-1) = -\frac{1}{q_0} \frac{dV(q)}{dq}\bigg|_{q_0} = \omega^{\ddagger 2} \Big(1 + \frac{3}{2} \frac{q_0}{q_1} \Big). \tag{B1}$$

so that in the weak damping limit the kink point is at $q_0 = \frac{q_1}{3}$.

In the overdamped limit, when $\alpha \to \infty$ one finds that $A \simeq \lambda^\ddagger \simeq \frac{\omega^\ddagger}{2\alpha}$ and $C \simeq 2^{\frac{3}{2}}\alpha$. In this case, the integral in Eq. (2.25) can be estimated as $\frac{1}{\beta A^2 C(q_0 + \frac{q_1}{9})}$ and Eq. (2.25) is

$$A^2 C^2 \Big(q_0 + \frac{q_1}{9} \Big) = -\frac{dV(q)}{dq}\bigg|_{q_0} = \omega^{\ddagger 2} q_0 \Big(1 + \frac{3}{2} \frac{q_0}{q_1} \Big) \ . \tag{B2}$$

This leads to the strong damping estimate for the kink: $q_0 \simeq \frac{1 + (\frac{7}{3})^{\frac{1}{2}}}{3} q_1 \simeq 0.85 q_1$.

[1] H.A. Kramers, Physica **7**, 284 (1940).

[2] H. Risken, *The Fokker-Planck Equation* (Springer, Berlin 1989).

[3] P. Hänggi, P. Talkner, and M. Borkovec, Rev. Mod. Phys. **62**, 251 (1990).

[4] B.J. Berne, M. Borkovec, and J.E. Straub, J. Phys. Chem. **92**, 3711 (1988).

[5] R.F. Grote and J.T. Hynes, J. Chem. Phys. **73**, 2715 (1980).

[6] K. Lindenberg and V. Seshadri, Physica A **109**, 483

(1981).
[7] K. Lindenberg and E. Cortés, Physica A **126**, 489 (1984).
[8] B. Carmeli and A. Nitzan, Chem. Phys. Lett. **102**, 517 (1983).
[9] A.M. Frishman and E. Pollak, J. Chem. Phys. **96**, 8877 (1992).
[10] A.M. Frishman and E. Pollak, J. Chem. Phys. **98**, 9532 (1993).
[11] J.B. Straus and G.A. Voth, J. Chem. Phys. **96**, 5460 (1992).
[12] J.B. Straus, J.M. Gomez Llorente, and G.A. Voth, J. Chem. Phys. **98**, 4082 (1993).
[13] E. Pollak, J. Chem. Phys. **85**, 865 (1986).
[14] E. Pollak, S.C. Tucker, and B.J. Berne, Phys. Rev. Lett. **65**, 1399 (1990).
[15] E. Pollak, J. Chem. Phys. **93**, 1116 (1990).
[16] R. Zwanzig, J. Stat. Phys. **9**, 215 (1973).
[17] A.O. Caldeira and A.J. Leggett, Phys. Rev. Lett. **46**, 211 (1981); Ann. Phys. (N.Y.) **149**, 374 (1983).
[18] J.C. Keck, Adv. Chem. Phys. **13**, 85 (1967).
[19] P. Pechukas, in *Dynamics of Molecular Collisions, Part B*, edited by W.H. Miller (Plenum, New York, 1976), p. 269.
[20] E.P. Wigner, Trans. Faraday Soc. **34**, 29 (1938).
[21] E. Pollak, J. Chem. Phys. **95**, 533 (1991).
[22] A.M. Berezhkovskii, E. Pollak, and V. Yu. Zitserman, J. Chem. Phys. **97**, 2422 (1992).
[23] G.R. Haynes, G.A. Voth, and E. Pollak, Chem. Phys. Lett. **207**, 309 (1993).
[24] E. Pollak and P. Talkner, Phys. Rev. E **47**, 922 (1993).
[25] W.H. Miller, J. Chem. Phys. **61**, 1823 (1974).
[26] E. Pollak, J. Phys. Chem. **95**, 10235 (1991).